Physica B 403 (2008) 3424–3428

Contents lists available at ScienceDirect

Physica B

journal homepage: www.elsevier.com/locate/physb

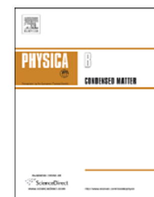

Raman characterization of hydrogen ion implanted silicon: "High-dose effect"?

Sergey V. Ovsyannikov [a,b,*], Vsevolod V. Shchennikov Jr [c], Vladimir V. Shchennikov [a], Yuri S. Ponosov [a], Irina V. Antonova [d], Sergey V. Smirnov [c]

[a] Institute of Metal Physics of Russian Academy of Sciences, Urals Division, GSP-170, 18 S. Kovalevskaya Str., Yekaterinburg 620041, Russia
[b] The Institute for Solid State Physics, The University of Tokyo, 5-1-5 Kashiwanoha, Kashiwa, 277-8581 Chiba, Japan
[c] Institute of Engineering Sciences of Russian Academy of Sciences, Urals Division, GSP-207, 34 Komsomolskaya Str., Yekaterinburg 620219, Russia
[d] Institute of Semiconductor Physics of Russian Academy of Sciences, Siberian Division, 13 Lavrentyeva Av., Novosibirsk, Russia

ARTICLE INFO

Article history:
Received 30 December 2007
Received in revised form
29 April 2008
Accepted 6 May 2008

PACS:
78.30.Ly
78.30.–j
78.30.Am
78.30.Fs
78.55.Ap
61.72.Tt
68.55.Ln

Keywords:
Silicon
Amorphous
Nanostructure
Hydrogen ion implantation
Raman spectra
High-dose effect

ABSTRACT

The Raman spectra of nanostructures formed on silicon Si single-crystalline wafers by implantation with hydrogen ions of fluencies ranging within $D\sim2\times10^{16}$–$3\times10^{17}\,cm^{-2}$ are reported. The presence of both crystalline and amorphous silicon phases were found in the spectra. A non-monotonic growth in the intensities of the peaks originating from the crystalline and the amorphous phases with a dose of the implantation was registered. A ratio of the intensities of the main peaks of the amorphous to the crystalline Si phases also demonstrated a non-monotonic behaviour ("high-dose effect"). Possible reasons and mechanisms of the non-monotonic dependence of a "degree" of amorphization on a dose of the implantation (or irradiation) are discussed.

© 2008 Elsevier B.V. All rights reserved.

1. Introduction

For many decades, the Si-H systems are of a steady interest owing to their scientific and technological importance [1–3]. While a solubility of hydrogen in crystalline silicon is quite low, an ion implantation technique permits introduction of hydrogen ions in high concentration [1–3]. High-dose implantation of silicon with low-energy hydrogen ions allows creating a layer, that contains hydrogenated silicon as well as crystalline and porous silicon phases [1,2]. This layer is characterized by (i) a high-temperature stability, (ii) a high hydrogen concentration (up to 20%), and (iii) a relatively low concentration of defects [1–3].

Implantation of silicon wafers with hydrogen ions is a basis of a number of modern micro- and nanotechnologies [2–6]. Thus, for instance, amorphous hydrogenated silicon (a-Si-H) is applied for manufacture of solar batteries [2]. On the other hand, under a two-stage thermal annealing (at 400–600 and above 1000 °C), the thin layer created on a surface of crystalline Si by H^+ implantation may be separated from the silicon wafer by microcracks along a platelet's sub-layer [3,7]. This peculiar property was put as a basis of the silicon-on-insulator (SOI) technologies, in which a thin silicon layer split from a wafer subjected to H^+ implantation (typically with a dose ranging within $\sim2\times10^{16}$–$1\times10^{17}\,cm^{-2}$) is attached to a silicon wafer capped by a film of SiO_2 [3]. Notice, that a high-pressure treatment above ~10 GPa also leads to cleavage of a sample of silicon containing atoms of interstitial oxygen into thin layers [8].

* Corresponding author at: Institute for Solid State Physics, The University of Tokyo, 5-1-5 Kashiwanoha, Kashiwa, 277-8581 Chiba, Japan. Tel.: +81 4 7136 3231; fax: +81 4 7136 3333.
E-mail addresses: sergey2503@gmail.com, sergey@issp.u-tokyo.ac.jp (S.V. Ovsyannikov).

0921-4526/$ - see front matter © 2008 Elsevier B.V. All rights reserved.
doi:10.1016/j.physb.2008.05.006

The ion-projected range is known to depend on energy of implanted ions [3], while a variation of H^+ doses was reported to result in differing nanostructures [1,9]. Atomic force microscopy images of silicon crystalline wafers implanted with H^+ doses ranging within $D\sim 1\text{–}6\times 10^{16}\,\mathrm{cm}^{-2}$ [10] demonstrate the effects of blistering and flaking of a surface and apparently show a strong dependence of a mesostructure of the surface on dose. Annealing of an implanted wafer was established to reduce a "degree of polymerization" (formation of three-dimensional structure from monomer molecules) of the Si-H bonds, which encourages production of both amorphous layers with nanocrystalline inserts and molecular hydrogen [1].

Hydrogenated wafers and films of crystalline and amorphous Si are intensively investigated by various techniques [1,6,7,10–17]. Since optical methods probe the short-range order in a substance, they are able to obtain information about local stresses, structural defects, fluctuations, and metastability of properties of hydrogenated layers [4,18]. In particular, Raman spectroscopy is a powerful tool for characterization of surface structure [4,12,19]. A numerous number of Raman studies have been already performed on hydrogenated crystalline and amorphous Si samples [1,4,11,12,14,19–23]. The majority of them were devoted to investigation of hydrogen-related defects and voids in Si, platelets (the ordered planar defects originating during accumulation of hydrogen of high concentration), and of the molecular form of hydrogen in Si.

Implantation (or irradiation) of crystalline Si with different ions or plasma was established to lead to a disordering of crystal structure, consisting in a partial amorphization of surface layer [24–30]. An increase in the amount of the amorphous phase with damage level was registered for doses lower than $\sim 10^{16}\text{–}10^{17}\,\mathrm{cm}^{-2}$ in a number of studies [24–28], whereas, implantation of higher doses was noticed to be able to reduce the amount of amorphous phase [24–28]. This implies that the tendency for growth of the amount of amorphous phase was broken by a recrystallization in a series of sequent implantations (irradiations) [24,25]. These phenomena were called the "high-dose effect" in the literature, and at present this effect has been registered in the silicon single-crystalline wafers implanted with P and B [24,25], As [26], Fe [27], and Si [28]. However, investigations of implantation effect on the Raman spectra of silicon are limited basically to low doses [22,23,29,31,32], and thereby the "high-dose effect" remains almost unstudied and not properly understood.

Hence a purpose of the present work was to perform a comparative characterization of a set of single-crystalline silicon wafers subjected to hydrogen ion implantation of different high doses (Table 1) by Raman spectroscopy. As Raman scattering is known to be an effective tool for probing layers in nanostructures, the spectra can give information about the phases of Si, which are probably formed in a surface layer on implantation with H^+, namely, amorphous, porous, nanocrystalline, and wurtzite Si as well as Si-H. The above-mentioned information would be useful for SOI and other micro-technologies [2–5].

Table 1
Doses of the hydrogen ion implantation of Si wafers

Sample	Dose of H^+ implantation (cm^{-2})	In the maximum of H distribution in Si	
		Si-H content (vol%)	Total volume of microcrystallites (vol%)
H1	2×10^{16}	39	35
H2	1.6×10^{17}	47	29
H3[a]	2×10^{17}	64	22
H4	3×10^{17}	71	16

[a] The wafer was additionally annealed at 500 °C for 30 min.

2. Experiment

A silicon wafer of (1 0 0) orientation was grown by the Czochralski technique (Cz-Si). Then, it was divided into several parts; each of them was subjected to implantation with hydrogen ions of different doses ranging within $2\times10^{16}\text{–}3\times10^{17}\,\mathrm{cm}^{-2}$ (Table 1). The implantation was accomplished with an assistance of a pulse source of ions with an energy of approximately 20 keV. During the implantation the intensity of fluency of hydrogen ions was kept at a low level in order to avoid heating of the wafers; hence the temperature of the wafers did not exceed 70 °C.

The Raman experiments were carried out on (0 0 1) planes of the silicon wafers in a backscattering geometry for both parallel $Z(XX)\overline{Z}$ and cross-polarization $Z(XY)\overline{Z}$ geometries (where Z—[0 0 1], X—[1 1 0], and Y—[$1\,\bar{1}\,0$]). The 514.5 nm line of an argon ion laser with power up to 5 mW was used for the Raman spectra excitation [33,34]. The collected spectra were analysed by a Renishaw microspectrometer. For the used exciting wavelength, the penetration depth of light inside crystal silicon is about 50 nm [35]. The laser beam was focused on a spot of 2–5 μm in diameter. The spectra obtained from different points of the wafers' surfaces gave similar results.

The hydrogen profiles verified by the secondary ion mass spectrometry [1] demonstrated that the concentration of hydrogen in the layer of thickness of 0.2 μm was about $10^{21}\text{–}10^{22}\,\mathrm{cm}^{-3}$ for H2 and H4 samples (Table 1). The ion-projected range depended on the dose of implantation and, for H1–H4 samples, ranged within 230–290 nm (Table 1). This layer consisted of silicon microcrystallites, amorphous Si, and voids filled with hydrogen. The increase in the ion's dose led to an increase in the concentration of the Si-H bonds inside this layer that resulted in a decrease in the total volume of the microcrystallites (Table 1). Annealing at 500 °C reduced the content of hydrogen at the maximum of its distribution along the projected range.

3. Results and discussion

The Raman spectra measured for both $Z(XX)\overline{Z}$ and $Z(XY)\overline{Z}$ polarization geometries on H1–H4 samples are shown in Fig. 1. The spectra show the characteristic features of both amorphous (a-Si; ~170, ~300, ~380, ~470, ~620–630, ~790–800, and ~950 cm^{-1}) [11], and crystalline (c-Si) phases of silicon (519.5 and ~970 cm^{-1}; Table 2). One can notice a growth in the intensities of the peaks which are assigned to a-Si and Si–H with a dose of the H^+ implantation (Fig. 2, inserts). An enhancement of the 520 cm^{-1} c-Si line intensity is also observed (Fig. 2, inserts). Similar but much weaker Raman spectra were earlier found in thin samples of a-Si [11]. However, the latter did not exhibit the second-order 2LO phonon peak near 800 cm^{-1}, which is known to be poorly observed in the Raman spectrum of a-Si. Whereas, some sorts of "treatments" of a material, for example, annealing with high power densities of an argon ion laser are able to enhance it [36]. Earlier, it was already noticed that an implantation with hydrogen ions enhances the intensity of the Raman spectrum of porous silicon films [21].

For the chosen orientation of the single-crystalline silicon wafer, (1 0 0), the phonon mode at ~520 cm^{-1} should not be visible in $Z(XY)\overline{Z}$ polarization geometry (Z—[0 0 1], X—[1 1 0], and Y—[$1\,\bar{1}\,0$]) [35]. Hence the manifestation of this phonon in the

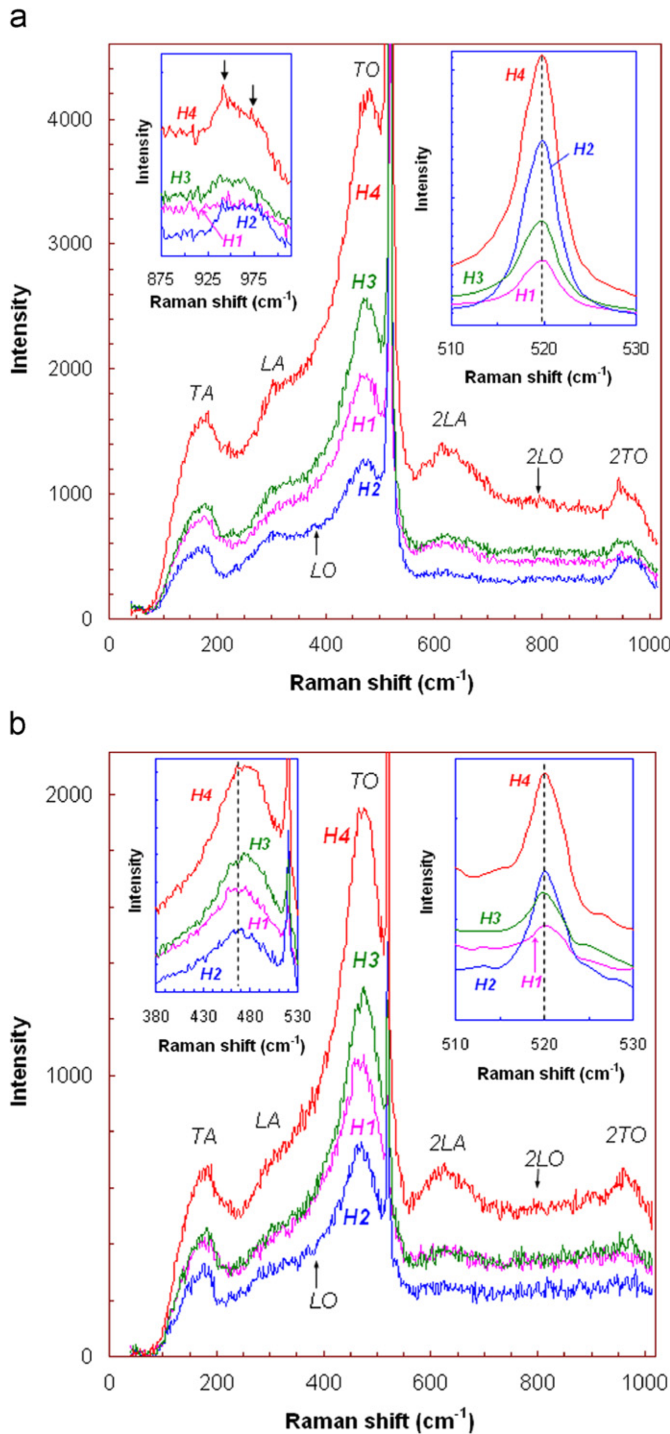

Fig. 1. Raman spectra of Si samples implanted with hydrogen ions (see Table 1), obtained at ambient conditions at $Z(XX)\bar{Z}$ (a) and $Z(XY)\bar{Z}$ (b) polarization geometries. In the right insets in (a) and (b) the peak of c-Si at 520 cm^{-1} is shown. In the left insets the doublet at ~960 cm^{-1} (a) and TO phonon of a-Si (b) are shown.

Table 2
Raman frequencies (cm^{-1}) of the Si wafers implanted with hydrogen ions, (Table 1) found for $Z(XX)\bar{Z}$ polarization geometry

Samples				Origin of the peak [11]	
1H	2H	3H	4H		
173	170	177	176	a-Si	TA[a]
308	298	299	301	a-Si	LA[a]
–	379	–	383	a-Si	LO[b]
473	472	474	477	a-Si	TO[a]
520	520	520	520	c-Si	LO[a]
625	621	629	628	a-Si	2LA[a]
799	–	–	800	a-Si	2LO[b]
948	944	944	947	a-Si	2TO[a]
972	977	965	973	c-Si	2TO[b]

(TA—transverse acoustic, LA—longitudinal coustic, TO—transverse optical, and LO—longitudinal acoustic phonons).
[a] At the centre of the Brillouin zone ($k = 0$).
[b] At the point $k \neq 0$.

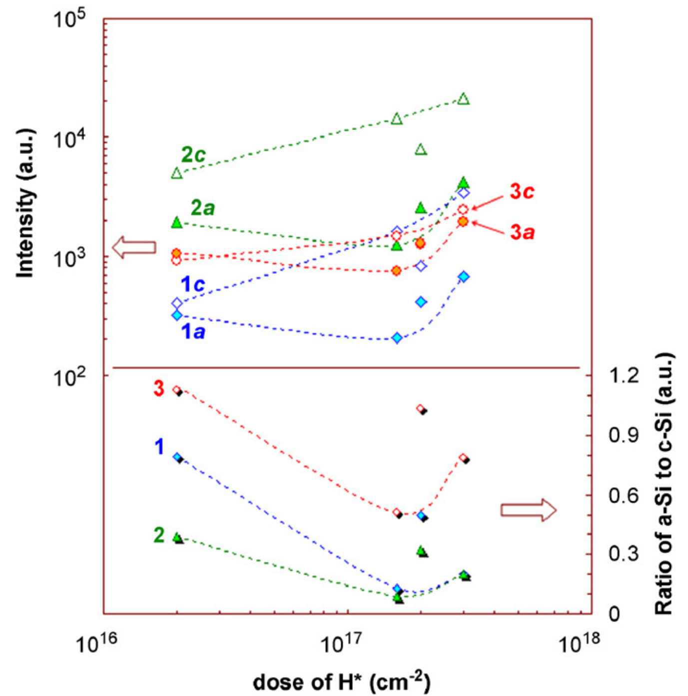

Fig. 2. Absolute (upper plot) and relative (lower plot) magnitudes of Raman intensities of the peak of crystalline silicon (c-Si) at 520 cm^{-1} and the one of hydrogenated and amorphous silicon (a-Si) at ~470 cm^{-1} versus dose of H$^+$ implantation (calculated from Fig. 1). The symbols 1 and 2 label the different series of experiments performed in $Z(XX)\bar{Z}$ polarization geometry; the series correspond to different points of a surface and various diameters of laser spots; 3—the data gathered in $Z(XY)\bar{Z}$ polarization geometry. The curves corresponding to a-Si and c-Si are marked, respectively, by a and c labels. The lower part of the plot shows a ratio of the amounts of the a-Si phase to the c-Si one, calculated from a ratio of the intensities of the main phonon peaks of a-Si to c-Si (from the upper part of the plot).

cross-polarization (Fig. 1b) might suggest polarization leakage or the presence of microcrystallites with a different orientation in the surface layer of the wafers, i.e. a partial change of the orientation of the surface after the implantation. Notice, that the intensities of the main phonon mode of c-Si at ~520 cm^{-1} for $Z(XX)\bar{Z}$ (allowed) polarization exceeded those for $Z(XY)\bar{Z}$ (forbidden) one by a factor of ~20 (Fig. 1). In the case of the peaks originating from the amorphous phase, their intensities were approximately equal for both the polarizations.

In order to perform a semi-quantitative analysis of influence of ion implantation level on the surface layer, we calculated the ratio of amounts of a-Si phase to the c-Si one from a ratio of the intensities of the main phonon peaks of a-Si at ~470 cm^{-1} to c-Si at ~520 cm^{-1} (Fig. 2). The intensities of the peaks of the other phonons of a-Si, such as: transverse acoustic (TA), longitudinal acoustic (LA), and longitudinal optical (LO) were less suitable for the above analysis, since earlier they were found to diminish with hydrogen content [11]. As, according to Ref. [11] the peak of a-Si at

$\sim$470 cm^{-1} did not show an appreciable variation in its intensity under implantation with hydrogen [11], its intensity may be directly related to the amount of the amorphous phase.

It is known that the absorption coefficient depends on the mesostructure: in amorphous and nanocrystalline silicon the coefficient is significantly higher than in c-Si (up to 15 times for 514.5 nm excitation) [37], while, in porous silicon it is lower than in c-Si [38]. Thus, the observed decrease in the ratio of amounts of a-Si to c-Si phases at low doses, and a simultaneous growth in the intensity of the peak at $\sim$520 cm^{-1} (Fig. 2) cannot be explained by changes in the absorption properties of the ion-projected range. Then, the behaviour of the peak intensity ratio (Fig. 2), suggesting a reduction in the amount of amorphous phase in a dose range 2×10^{16}–1.6×10^{17} cm^{-2}, apparently evidences the "high-dose effect" [24–27]. This seems to be the first observation of this effect in crystalline Si implanted with H$^+$. Under a further dose growth upto 3×10^{17} cm^{-2}, the amount of the amorphous phase slightly increased (Fig. 2). A significant growth in the amount of amorphous phase in H3 sample ($D=2\times10^{17}$ cm^{-2}) could arise owing to the annealing at 500 °C, which decreases the degree of polymerization and thereby "encourages" amorphization [1]. A study of the electrical characteristics of the nanostructures formed by implantation with close doses of H$^+$ also revealed a non-monotonic dependence on the dose [9].

Probably, the "high-dose effect" in Si implanted with H$^+$ arises owing to the enhancement of polymerization degree of Si-H bonds, and/or it may be related to radiation-induced recrystallization. In previous studies [24–28] limited and specified models of this effect were inferred. For example, Gerasimenko et al. [24] addressed the "high-dose effect" as a peculiar interaction between defects generated during the implantation process with impurities introduced. The model offered by Gerasimenko et al. [24] proposed an "epitaxial crystallization" of the amorphous phase, i.e. it stated that when the concentration of impurities reaches a certain level, they begin filling micropores and voids in the material [24]. However, it was also found that filling of micropores and voids inside a silicon wafer, with ions of inert gas Ar does not change the mesostructure of the wafer, and, hence, does not lead to recrystallization [24]. In work [25], the "high-dose effect" observed in silicon implanted with phosphorous was explained by a radiation-induced recrystallization of the amorphous phase by means of formation of chemical bonds with a lower energetic barrier, i.e. the Si–P bonds which are weaker than the Si–Si ones. Meanwhile, the latter hypothesis cannot explain recrystallization in self-implanted Si [28].

A process of implantation or irradiation may be generally viewed as a competition between damage production (amorphization) on the one hand and beam dynamic annealing leading to migration of defects (recrystallization) on the other hand [28]. Thus, the growth in the amount of amorphous phase we register at the dose $D=3\times10^{17}$ cm^{-2} (Fig. 2) indicates that the "damage" processes become dominating again. This circumstance points out the existence of the second threshold dose, and suggests a dependence of the threshold doses on temperature of implantation or irradiation.

Taking into account the existence of "high-dose effect" in single-crystalline Si implanted (or irradiated) with P, B, As, Fe, and Si [24–28], one may infer that the above non-monotonic dependence of the amount of amorphous phase on dose of implantation or irradiation is probably a typical feature for silicon single-crystalline wafers as well as for some other materials. The regularity consists in the existence of two threshold doses; (i) until the first one, the amount of amorphous phase grows with dose ("low-dose regime"); (ii) after passing the first threshold and until the second one, the amount of amorphous fraction diminishes with dose owing to the "recrystallization" phenomena ("high-dose effect"); (iii) after passing the second threshold dose, the amount of amorphous phase increases with dose again (Fig. 2). The threshold doses probably depend on the nature of wafer and implantant. Temperature conditions of implantation (irradiation) process should influence them as well. One cannot also exclude the existence of other phenomena at much higher doses.

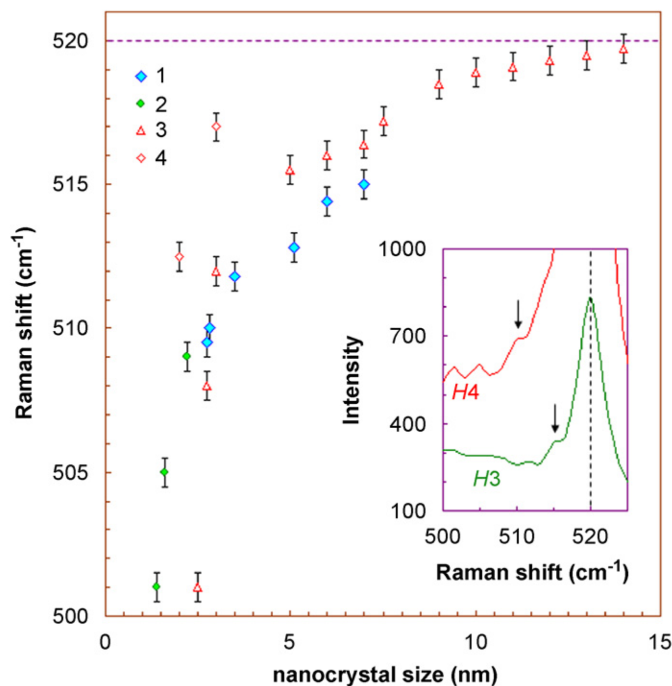

Fig. 3. The dependence of frequency of the first-order LO phonon of nanocrystalline Si on a size of crystallites, 1—from Ref. [36], 2—from Ref. [40], 3 and 4—from Ref. [41]. According to calculations [39], a difference in shapes of nanocrystallites leads to a variation in the dependence only when characteristic sizes are less than $\sim$3 nm. In the inset, a peculiarity at $\sim$510–515 cm^{-1} in the left shoulder of the main peak of c-Si is shown; the spectra were excited with low laser powers in $Z(XX)\overline{Z}$ polarization geometry.

Fig. 3 summarizes the observed frequencies of c-Si phonon at 520 cm^{-1} in nanocrystalline Si versus a typical size of nanocrystallites, extracted from the Raman spectra shown in Refs. [36,39–41]; a formula for precise calculation of its frequency is given, for example, in Ref. [36]. An asymmetric shape of the phonon peak at $\sim$520 cm^{-1} that we established in our spectra (Fig. 1a, insert), potentially may hint at the presence of Si nanocrystallites [36,39–41], porous Si [5,32,42–44], and wurtzite Si [5,45]. In our experiments we did not observe any noticeable softening or clear splitting of this main crystalline peak (Fig. 1). Therefore, either characteristic sizes of pores or nanocrystallites were basically larger than $\sim$15–20 nm (Fig. 3), or only negligible (for Raman detection) amount was formed under the implantation. Thus, implantation with hydrogen ions does not lead to the appearance of nanocrystalline or wurtzite silicon. Meanwhile, in some spectra excited with low laser powers ($\sim$1 mW), we observed a tiny peculiarity at $\sim$510–515 cm^{-1} in the left shoulder of the main peak of c-Si (Fig. 3, insert). This feature potentially might be addressed either to nanocrystallites of a certain size (Fig. 3) or to the wurtzite form of Si [5,45]. However, since this tiny peak is comparable to the background and thereby could not be reliably resolved, it may not serve as an evidence.

4. Conclusion

The Raman spectra of single-crystalline wafers of Si implanted with various doses of H$^+$ ions revealed the presence of both

crystalline and amorphous Si. The behaviour of the ratio of the peak intensities at ~470 (a-Si) and ~520 cm^{-1} (c-Si) evidences a non-monotonic dose dependence of the amount of amorphous phase of silicon in the ion-projected range. The literature data also reported about an increase in the amount of amorphous phase with dose of implantation or irradiation at low doses [24–28]. Thus, the obtained dependence hints at two crossover points; (i) after passing the first one the amount of amorphous phase decreases with dose; (ii) and after passing the second one, the amount of amorphous phase grows with dose again. The existence of the first crossover has been already established in single-crystalline silicon implanted with P, B [20,25], As [26], Fe [27], and self-implantation [28]. A question arises as to whether the "high-dose effect" is a typical feature for silicon single-crystalline wafers and some other materials. No obvious traces of the presence of nanocrystalline, porous, or wurzite silicon in the implanted wafers were observed in the Raman spectra. The results obtained seem to be useful for manufacture of SOI structures and for other implantation technologies. They also demonstrate the applicability of Raman spectroscopy for characterization of Si-based nanostructures.

Acknowledgements

The authors are grateful to Dr. I.I. Morozov (ISP) for the hydrogen implantation. The work was supported by the Russian Foundation for Basic Research. S.V.O. thanks the Japanese Society for the Promotion of Science and the Institute for Solid State Physics for financial support. The authors are also grateful to the referees for the careful reading of the manuscript and for valuable comments and suggestions.

References

[1] V.P. Popov, I.V. Antonova, A.K. Gutakovsky, E.V. Spesivtsev, I.I. Morosov, Mater. Sci. Eng. B 73 (2000) 120;
V.P. Popov, I.E. Tyschenko, L.N. Safronov, O.V. Naumova, I.V. Antonova, A.K. Gutakovsky, A.B. Talochkin, Thin Solid Films 403 (2002) 500.
[2] B. Kramer (Ed.), Advances in Solid State Physics, vol. 44, Springer, Berlin Heidelberg, 2004.
[3] M. Bruel, Electron. Lett. 31 (1995) 1201;
M. Bruel, Nucl. Instr. and Meth. B 108 (1996) 313.
[4] P. Danesh, B. Pantchev, D. Grambole, B. Schmidt, J. Appl. Phys. 90 (2001) 3065.
[5] Z.H. Hu, X.B. Liao, H.W. Diao, Y. Cai, S.B. Zhang, E. Fortunato, R. Martins, J. Non-Cryst. Solids 352 (2006) 1900.
[6] J. Ciosek, J. Ratajczak, Appl. Surf. Sci. 252 (2006) 6115.
[7] N. Sousbie, L. Capello, J. Eymery, F. Rieutord, J. Appl. Phys. 99 (2006) 103509.
[8] V.V. Shchennikov, et al., Tech. Phys. Lett. 29 (2003) 598.
[9] O.V. Naumova, I.V. Antonova, V.P. Popov, V.F. Stas', Semiconductors 37 (2003) 92;
O.V. Naumova, I.V. Antonova, V.P. Popov, V.F. Stas', Microelectron. Eng. 66 (2003) 422.
[10] O. Moutanabbir, B. Terreault, M. Chicoine, F. Schiettekatte, Appl. Phys. A 80 (2005) 1455.
[11] D. Bermejo, M. Cardona, J. Non-Cryst. Solids 32 (1979) 405.
[12] E.V. Lavrov, J. Weber, Phys. Rev. Lett. 87 (2001) 185502;
E.V. Lavrov, J. Weber, Phys. Rev. Lett. 89 (2002) 215501;
E.V. Lavrov, J. Weber, Physica B 308 (2001) 151.
[13] B. Pantchev, P. Danesh, I. Savatinova, E. Liarokapis, B. Schmidt, D. Grambole, J. Phys. D 34 (2001) 2589.
[14] Y. Ma, Y.L. Huang, W. Dungen, R. Job, W.R. Fahrner, Phys. Rev. B 72 (2005) 085321.
[15] S.V. Ovsyannikov, V.V. Shchennikov, I.V. Antonova, V.V. Shchennikov Jr., S.N. Shamin, Phys. Solid State 48 (2006) 47.
[16] S.V. Ovsyannikov, V.V. Shchennikov Jr., N.A. Shaydarova, V.V. Shchennikov, et al., Physica B 376–377 (2006) 177.
[17] S.V. Ovsyannikov, V.V. Shchennikov, I.V. Antonova, V.V. Shchennikov Jr., Y.S. Ponosov, Mater. Sci. Eng. A 462 (2007) 343.
[18] S.C. Agarwal, J. Mater. Sci. Mater. Electron. 14 (2003) 703.
[19] S.V. Ovsyannikov, V.V. Shchennikov, A. Cantarero, A. Cros, A.N. Titov, Mater. Sci. Eng. A 462 (2007) 422.
[20] J.F. Morhange, G. Kanellis, M. Balkanski, Solid State Commun. 31 (1979) 805.
[21] W.J. Salcedo, E.E. Peres, F.J.R. Fernandez, J.C. Rubim, Vibr. Spectrosc. 36 (2004) 135.
[22] A. Pan, Y.L. Wang, C.S. Wu, C.D. Chen, N.W. Liu, J. Vacuum Sci. Technol. B 23 (2005) 2288.
[23] W. Dungen, R. Job, Y. Ma, Y.L. Huang, W.R. Fahrner, L.O. Keller, J.T. Horstmann, Solid State Phenom. 108–109 (2005) 91.
[24] N.N. Gerasimenko, A.V. Dvurechenskii, S.I. Romanov, L.S. Smirnov, Sov. Phys. Semicond.-USSR 6 (1973) 1692;
N.N. Gerasimenko, A.V. Dvurechenskii, S.I. Romanov, L.S. Smirnov, Sov. Phys. Semicond.-USSR 7 (1974) 1461.
[25] D.I. Tetelbaum, A.I. Gerasimov, Semiconductors 38 (2004) 1260.
[26] H. Sano, J. Saito, J. Ikeda, G. Mizutani, J. Appl. Phys. 100 (2006) 043710.
[27] D.A. Zatsepin, E.S. Yanenkova, E.Z. Kurmaev, V.M. Cherkashenko, S.N. Shamin, S.O. Cholakh, Phys. Solid State 48 (2006) 218;
D.A. Zatsepin, E.Z. Kurmaev, I.R. Shein, V.M. Cherkashenko, S.N. Shamin, S.O. Cholakh, Phys. Solid State 49 (2007) 75.
[28] X.F. Zhu, J.S. Williams, J.C. McCallum, Nucl. Instr. and Meth. B 148 (1999) 268.
[29] R. Prabakaran, G. Raghavan, S.T. Sundari, R. Kesavamoorthy, Solid State Commun. 133 (2005) 801.
[30] M. Sadiq, M. Shafiq, A. Waheed, R. Ahmad, M. Zakaullah, Phys. Lett. A 352 (2006) 150.
[31] J.C.N. Reis, A.F. Beloto, M. Ueda, Nucl. Instr. and Meth. B 240 (2005) 219.
[32] R. Prabakaran, R. Kesavamoorthy, S. Amirthapandian, A. Ramanand, Mater. Lett. 58 (2004) 3745.
[33] S.V. Ovsyannikov, Y.S. Ponosov, V.V. Shchennikov, V.E. Mogilenskikh, Phys. Status Solidi (c) 1 (2004) 3110.
[34] S.V. Ovsyannikov, V.V. Shchennikov, Y.S. Ponosov, S.V. Gudina, V.G. Guk, E.P. Skipetrov, V.E. Mogilenskikh, J. Phys. D 37 (2004) 1151.
[35] J.L. Birman, Theory of Crystal Space Groups and Infra-Red and Raman Lattice Processes of Insulating Crystals, Springer, Berlin–Heidelberg–New York, 1974.
[36] P. Mishra, K.P. Jain, Phys. Rev. B 62 (2000) 14790;
P. Mishra, K.P. Jain, Phys. Rev. B 64 (2001) 073304;
P. Mishra, K.P. Jain, Mater. Sci. Eng. B 95 (2002) 202.
[37] S.B. Korovin, A.N. Orlov, A.M. Prokhorov, V.I. Pustovoi, M. Konstantaki, S. Couris, E. Koudoumas, Quantum Electron. 31 (2001) 817.
[38] M.E. Kompan, I.I. Novak, V.B. Kulik, N.A. Kamakova, Phys. Solid State 41 (1999) 1207.
[39] J. Zi, H. Buscher, C. Falter, W. Ludwig, K.M. Zhang, X.D. Xie, Appl. Phys. Lett. 69 (1996) 200.
[40] R.K. Soni, L.F. Fonseca, O. Resto, M. Buzaianu, S.Z. Weisz, J. Lumin. 83–4 (1999) 187.
[41] G. Faraci, S. Gibilisco, P. Russo, A.R. Pennisi, S. La Rosa, Phys. Rev. B 73 (2006) 033307.
[42] S. Trusso, C. Vasi, M. Allegrini, F. Fuso, G. Pennelli, J. Vacuum Sci. Technol. B 17 (1999) 468.
[43] E. Galeazzo, W.J. Salcedo, H.E.M. Peres, F.J. Ramirez-Fernandez, Sensors Actuators B 76 (2001) 343.
[44] M.N. Islam, S. Kumar, Appl. Phys. Lett. 78 (2001) 715.
[45] J. Bandet, B. Despax, T. Caumont, J. Phys. D 35 (2002) 234.